Can an Ab-Initio Three-Body Virial Equation Describe the Mercury Gas Phase?

ARTICLE *in* THE JOURNAL OF PHYSICAL CHEMISTRY B · FEBRUARY 2014

Impact Factor: 3.3 · DOI: 10.1021/jp412260a · Source: PubMed

5 AUTHORS, INCLUDING:

Elke Pahl

Massey University

27 PUBLICATIONS **398** CITATIONS

SEE PROFILE

Peter Schwerdtfeger

Massey University

339 PUBLICATIONS **8,310** CITATIONS

SEE PROFILE

THE JOURNAL OF PHYSICAL CHEMISTRY B

Article

pubs.acs.org/JPCB

Can an Ab Initio Three-Body Virial Equation Describe the Mercury Gas Phase?

J. Wiebke,*[,†] M. Wormit,[‡] R. Hellmann,[§] E. Pahl,[†] and P. Schwerdtfeger*[,†]

[†]Centre for Theoretical Chemistry and Physics, The New Zealand Institute for Advanced Study and Institute of Mathematical and Natural Sciences, Massey University Albany, Private Bag 102904, Auckland 0745, New Zealand

[‡]Interdisciplinary Center for Scientific Computing, Universität Heidelberg, Im Neuenheimer Feld 368, D-69120 Heidelberg, Germany

[§]Institut für Chemie, Universität Rostock, Albert-Einstein-Straße 3a, D-18059 Rostock, Germany

Supporting Information

ABSTRACT: We report a sixth-order ab initio virial equation of state (EOS) for mercury. The virial coefficients were determined in the temperature range from 500 to 7750 K using a three-body approximation to the *N*-body interaction potential. The underlying two-body and three-body potentials were fitted to highly accurate Coupled-Cluster interaction energies of Hg_2 (Pahl, E.; Figgen, D.; Thierfelder, C.; Peterson, K. A.; Calvo, F.; Schwerdtfeger, P. *J. Chem. Phys.* **2010**, *132*, 114301-1) and equilateral-triangular configurations of Hg_3. We find the virial coefficients of order four and higher to be negative and to have large absolute values over the entire temperature range considered. The validity of our three-body, sixth-order EOS seems to be limited to small densities of about 1.5 g cm^{-3} and somewhat higher densities at higher temperatures. Termwise analysis and comparison to experimental gas-phase data suggest a small convergence radius of the virial EOS itself as well as a failure of the three-body interaction model (i.e., poor convergence of the many-body expansion for mercury). We conjecture that the *n*th-order term of the virial EOS is to be evaluated from the full *n*-body interaction potential for a quantitative picture. Consequently, an ab initio three-body virial equation cannot describe the mercury gas phase.

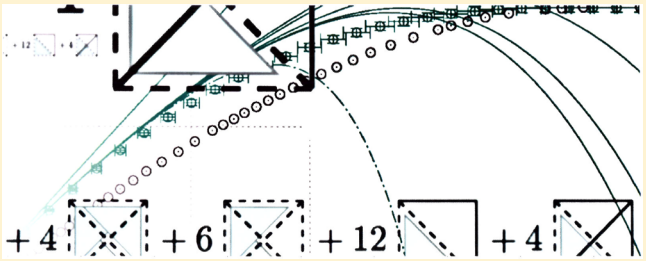

1. INTRODUCTION

Among the elements of the periodic table, mercury (^{80}Hg) exhibits many peculiarities. Whereas it is a typical transition metal characterized by rich group XVI and XVII chemistry[1] and a range of metallic solid phases,[1,2] the location of mercury's phase diagram in the pressure−temperature plane is striking. Hg is the only metal liquid under ambient conditions: at atmospheric pressure, the (rhombomedral α-Hg) solid melts at 234.3 K to form a conducting liquid.[3] In view of the fact that mercury evaporates at 629.81 K[3] and undergoes a metal-to-insulator transition in the vicinity of the coexistence point,[4−6] the domain of thermodynamic stability of mercury's liquid phase is exceptionally small. Likewise, its liquid−vapor critical temperature of 1751 K[4,5] is believed to be the lowest of all metals. This peculiar phase behavior is understood to arise from a strong relativistic stabilization of the filled 6s subshell,[7−9] rendering Hg a comparatively weakly interacting "pseudonoble gas".[7] Although we will illustrate that the idea of a pseudonoble gas is somewhat far-fetched,[8,10] mercury is indeed believed to be the only metal forming a monatomic, van der Waals-interacting dilute gas phase.[7]

It is therefore interesting to ask if the equation of state (EOS) of the Hg gas phase can be formulated as a virial series

$$P(\rho, T) = k_B T \rho \left[1 + \sum_{n=2}^{\infty} B_n(T) \rho^{n-1} \right] \quad (1)$$

truncated after some order *m*. Therein *P*, ρ, and *T* are the pressure, number density, and temperature, respectively; k_B is Boltzmann's constant. In Mayer et al.'s cluster expansion of the grand canonical partition function,[11,12] virial coefficients B_n arise as functionals of the interaction potential *E* of *n* atoms. Generally, for *N* particles, *E* can be written as[11]

$$E(\mathbf{R}^N) = \sum_{v=2}^{N} E_v(\mathbf{R}^N) = \sum_{v=2}^{N} \left[\sum_{i_1 < \cdots < i_v} \Phi_{i_1 \cdots i_v} \right] \quad (2)$$

where $\Phi_{i_1 \ldots i_v} = \Phi_v(\mathbf{r}_{i_1}, \ldots \mathbf{r}_{i_v})$ is a *v*-body potential[11] and $\mathbf{R}^N$ collects all *N* particle position vectors $\mathbf{r}$. Therefore, although eq 1 implies the limit $N \to \infty$, B_n is a functional of the terms in eq 2 up to and including order *n* only. Recent reformulations[13,14] of Mayer et al.'s[11] (and later Ree's and Hoover's[15]) diagrammatic schemes significantly reduce the number of diagrams required to evaluate the B_n coefficients numerically and have been coupled to sophisticated Monte Carlo

Received: December 15, 2013
Revised: February 9, 2014
Published: February 18, 2014

   dx.doi.org/10.1021/jp412260a | *J. Phys. Chem. B* 2014, 118, 3392−3400

integrators.[14,16,17] Consequently, for systems with many-body expansions of the interaction energy E converging reasonably fast, virial coefficients and EOSs have been reported to rather high orders,[14,17−23] most notably up to order 5 for H_2O,[18] up to 7 for Ar from ab initio two- and three-body potentials,[19] up to 8 for a Lennard-Jones system,[17,20] and up to order 10 and 12 for a soft-core and hard-core model, respectively.[14,21,22] We note in passing that the regime of applicability of eq 1 is suggested to be more strongly restricted than by the (generally unknown) radius of convergence of the density expansion alone.[24,25] However, for prototypical systems such as Ar, this regime is sufficiently large for a seventh-order ab initio virial EOS of Ar to reproduce a range of bulk properties to remarkable accuracy.[19,26,27]

Our motivation for the work reported here is at least twofold. First, a number of simple parametrizations of the low-density vapor EOS have been reported as (formally) second-order virial EOSs,[28−30] usually collecting non-ideality corrections in a term $k_B T\tilde{B}_2\rho^2$ with $\tilde{B}_2 \propto 1/T^2$. The possibility of the density expansion of eq 1 also seems to be taken for granted in more recent works.[31,32] However, we feel that, for mercury, the entire idea of fitting polynomials in ρ to experimental $P-\rho-T$ data is invalid on physical grounds (although, of course, well-grounded analytically). Whereas the formation of the smallest Hg_N clusters is driven by dispersion interaction, larger clusters exhibit covalent bonding characteristics and, for even larger N, have strongly delocalized electronic structures indicative of metals.[8,10,33] Consequently, eq 2 converges extremely slowly for Hg_N. Even for moderate N the N-particle interaction potential is not well approximated by the pairwise-additive contribution $\Sigma_{i<j}\,\Phi_{ij}$, in stark contrast to the prototypical van der Waals-interacting rare gases.[1,19,34] Although we are not going to give a rigorous proof, we expect poor convergence of eq 2—understanding convergence to be $|E_\nu| \ll |E_{\nu-1}|$ for $3 \le \nu \le N$—to effect a breakdown of the density expansion of eq 1. Second, to the best of our knowledge, this idea has never been put to the test. In short, we believe that an ab initio virial EOS cannot describe the mercury gas phase.

We point out that questions regarding the gas-phase behavior of mercury are of dire importance from the point of view of significant antropogenic mercury emissions into the atmosphere[35,36] and the high toxicity of mercury.[37] However, whereas Götzlaff et al. reported accurate and extensive discrete $P-\rho-T$ measurements,[4,5] no smooth, accurate EOS for the mercury gas phase is known. For reasons outlined above, we cannot hope to establish such an equation here. It is nevertheless intriguing to ask the following questions. Can eq 1, truncated at some order, describe the low-density gas phase of mercury? If so, to which extent? Is it possible to identify a regime of applicability? How, quantitatively and qualitatively speaking, does eq 1 fail outside that regime?

Here we address these and other questions by constructing a sixth-order approximation to the virial series of eq 1 from ab initio two- and three-body potentials. This approach is not meant to be the most accurate possible. Instead, it allows a discussion in terms of quantities with clear, physical interpretations. Our article is organized as follows. In section 2 we present the ab initio three-body interaction model and the protocol employed to compute the virial coefficients B_2 to B_6. In sections 3 and 4 we discuss the T dependence of the virial coefficients, summation of terms $k_B T B_n \rho^n$, and ab initio EOS data derived. We will compare with experimental data[4,5,28−30] and frequently consider argon (which has recently been investigated using a very similar ab initio approach[19]) as a real rare gas. In section 5, we then attempt a critical discussion of our approach and the adequacy of our interaction model in particular. Section 6 concludes and presents a perspective on future work.

2. INTERACTION MODEL AND COMPUTATIONAL DETAILS

Our ab initio mercury interaction model is defined by truncating the many-body expansion of eq 2 at third order: $E \approx E_2 + E_3$. We employ our ab initio Extended Lennard-Jones (ELJ) potential[38]

$$\Phi_{ij} = \Phi_2(\mathbf{r}_i, \mathbf{r}_j) = \sum_{t=6}^{14} \frac{a_t}{|\mathbf{r}_i - \mathbf{r}_j|^t} \tag{3}$$

for the two-body part E_2. The coefficients a_t have been fitted to a Hg_2 potential energy curve calculated on a CCSD(T) (i.e., Coupled Cluster up to single, double, and noniterative triple excitations) level of theory and including spin−orbit and full triple corrections as detailed in ref 38. The three-body contribution E_3 is parametrized to fit (a subset of) an ab initio potential energy surface of the mercury trimer Hg_3 as described below.

Similar to refs 39 and 40, we will frequently refer to the nth virial coefficient B_n as a sum of ν-body parts B_{n_ν} such that $B_n = \Sigma_{\nu=2}^{n} B_{n_\nu}$ with $B_{n_\nu} = B_n(\{\Phi_\mu\}_{\mu=2}^{\nu}) - B_n(\{\Phi_\mu\}_{\mu=2}^{\nu-1})$. From this point of view, our three-body interaction model gives rise to three-body approximations $B_{n_2} + B_{n_3}$ for the fourth- and higher-order virial coefficients.

2.1. Hg_3 Potential Energy Surface. The ab initio potential energy surface (PES) of the mercury trimer Hg_3 has been computed at the CCSD(T) level of theory as implemented in, and using, the Molpro program suite.[41] We used the scalar-relativistic small-core pseudopotential of Figgen et al.[42] and the corresponding hierarchy of aug-cc-pVxZ-PP basis sets[43] with $x \in \{D, T, Q, 5\}$. The total energies of Hg_3, as well as of all Hg_2 and Hg fragments computed in the full trimer basis, have been extrapolated to the complete basis set (CBS) limit using a two-point ansatz[44] with the QZ and 5Z energies.

2.2. Three-Body Potentials. Given the ab initio Hg_3 PES, we obtain analytical three-body potentials Φ_3^X as follows. We consider the three-body part $\mathcal{E}_3$ intrinsic to the Hg_3 PES,

$$\mathcal{E}_3(\mathbf{R}^3) = \mathcal{E}(\mathbf{R}^3) - \mathcal{E}(\mathbf{r}_1, \mathbf{r}_2) - \mathcal{E}(\mathbf{r}_1, \mathbf{r}_3) - \mathcal{E}(\mathbf{r}_2, \mathbf{r}_3) + \mathcal{E}(\mathbf{r}_1) + \mathcal{E}(\mathbf{r}_2) + \mathcal{E}(\mathbf{r}_3)$$

for equilateral configurations (i.e., for $r_{12} \equiv r_{13} \equiv r_{23} \equiv r$ between $3.75a_0$ and $50a_0$, where a_0 is the Bohr radius). Therein $\mathcal{E}$ is a CBS-extrapolated CCSD(T) energy in the full atom-centered trimer basis for the three-body configuration $\mathbf{R}^3 = (\mathbf{r}_1, \mathbf{r}_2, \mathbf{r}_3)$. We fit

$$\Phi_3^X(\mathbf{R}^3) = \omega_{ddd} f_\theta(\mathbf{R}^3)\left[\frac{1}{r_{12}^3 r_{13}^3 r_{23}^3} + f_r^X(\mathbf{R}^3)\right] \tag{4}$$

with the triple-dipole angular function $f_\theta(\mathbf{R}^3) = 1 + 3\cos\theta_{12}\cos\theta_{13}\cos\theta_{23}$ to the equilateral $\mathcal{E}_3(r)$ data using standard least-squares techniques and a uniform weighting of points. We begin with $f_r^{AT} \equiv 0$; then Φ_3^{AT} is of the triple-dipole Axilrod−Teller−Muto form. Fitting Φ_3^{AT} to $\mathcal{E}_3(r)$ between $12.5a_0$ and $50a_0$, where $\mathcal{E}_3$ is dominated by the long-range dispersion

dx.doi.org/10.1021/jp412260a | J. Phys. Chem. B 2014, 118, 3392−3400

component (i.e., where the Hartree−Fock part is negligible in comparison), we obtain $\omega_{ddd} = 8.18327 \times 10^3 E_h a_0^9$. Fixing this parameter, we then fit an Extended Axilrod−Teller form[46] Φ_3^{EAT} to the short-range correction $f_r^{EAT}(\mathbf{R}^3) = e^{-\alpha\bar{r}} \Sigma_t \beta_t R^t$, where $3\bar{r} = r_{12} + r_{13} + r_{23}$ and $R = (r_{12} r_{13} r_{23})^{1/3}$, to the $\mathcal{E}_3(r)$ data between $5.7a_0$ and $28.3a_0$. Over the range $5.7a_0 \le r \le 50.0a_0$, we achieve a fit with a rms error of about $5 \times 10^{-5} E_h$ (and somewhat larger rms deviations if yet smaller values of r are included). The resulting values of α and β_t are given in the Supporting Information.

We note in passing that the functional form of eq 4 is approximate. Both the EAT and AT forms employ the triple-dipole angular function f_θ whereas the exact three-body potential must be expected to have a different dependence on θ_{12}, θ_{13}, and θ_{23} for small Hg−Hg separations.[19,47,48] However, at least for the virial coefficients B_2, B_3, and B_4 of Ar, a well-parametrized EAT form[46] is an excellent approximation[39,40] to a very accurate three-body potential.[19,48]

Figure 1 plots the potential energy per atom (i.e., $E(r)/3 = \Phi_2(r) + \Phi_3(r)/3$) of the equilateral Hg_3 system as a function of the Hg−Hg separation r. For a pairwise-additive interaction model, $E \approx E_2$, this coincides with the potential energy curve of the dimer. Thus, Figure 1 illustrates the importance of the next-higher term in the many-body expansion of the interaction potential (i.e., the three-body part). In this equilateral picture, Φ_3^{EAT} both softens and strengthens the ELJ potential. The effect is already pronounced at reduced equilateral Hg−Hg separations of $r/\sigma_{Hg} = 1.25$ (about $7.5a_0$) and of the same order of magnitude as the ELJ potential's well depth ε_{Hg} for the repulsive branch $r < \sigma_{Hg}$ of the two-body potential. Here, $\sigma_{Hg} = 5.927a_0$[38] is the Hg−Hg distance where the two-body potential vanishes. The resulting great difficulties in parametrizing effective Lennard-Jones potentials are well documented.[49−51] Note that the reduced Hg_2 potential[38] is already significantly less repulsive in the repulsive branch and less steep in the outer well region than the Ar_2 potential.[45] (The two-body and three-body potential curves of argon are indistinguishable on the scale of Figure 1.)

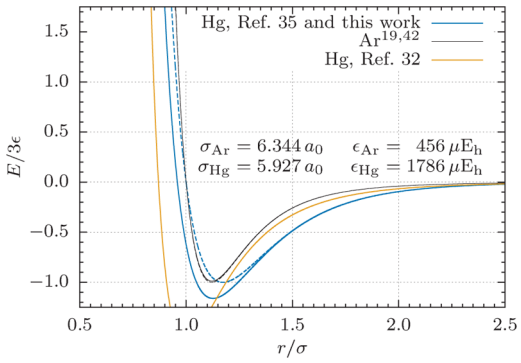

Figure 1. Potential energy per atom, $E(r)/3$, in the equilateral mercury trimer as a function of the Hg−Hg separation r. Also shown is the analogous Ar_3 system. All quantities are reduced by the respective two-body potential's[38,45] σ and ε values; dashed curves illustrate the respective pairwise-additive approximations $E \approx E_2$. Also shown is the reduced effective Hg_2 potential of Fokin et al.[32]

2.3. Computing the Virial Coefficients. The virial coefficients B_2 to B_6 have been computed following Hellmann and Bich[13] and using the Mayer sampling approach of Singh and Kofke.[13,16,19] Briefly, Mayer sampling refers to a biased n-particle Markov chain Monte Carlo (MC) method to numerically evaluate B_n relative to B_n for a reference system.[16] Here, as elsewhere,[16,19] we choose the hard-sphere model (with temperature-independent hard-sphere virial coefficients by Clisby and McCoy[21]) as a reference.

Given a combination of our ELJ two-body and either the AT or EAT three-body potentials, the B_n coefficients have been computed as follows. We define[16,19] the reference system's hard-sphere diameter as $\sigma_{Hg} = 5.927a_0$. We consider only configurations with separations from the center of mass of less than $18\,897a_0$ (about 10 000 Å). For Hg−Hg separations smaller than $3.75a_0$, we set the three-body potential to zero, and for separations smaller than a_0, the two-body Mayer functions are replaced by those of overlapping hard spheres. We then obtain B_n as an average over 9 statistically independent runs of 10^{10} MC cycles each, using a multitemperature sampling protocol similar to that in ref 19. We evaluate B_2 to B_6 at temperatures of 500, 629.81, and 750 K and at an additional 28 equally spaced temperatures T_τ in the 1000−7750 K range. Using the two-standard deviation of the mean as an error estimate, this protocol determines B_2, B_3, and B_4 to relative accuracies much better than ±1% (and somewhat worse near zero crossings). B_5 and B_6 are computed to inferior accuracy with worst-case relative errors of ±2 and ±13%, respectively, near 2000 K. Kirkwood−Wigner quantum corrections to first order in $\hbar^2$ have been found to be insignificant for B_2 at all temperatures of interest and have therefore been neglected for all B_n.

The variability of particularly the higher-order virial coefficients B_n with temperature T is such that fitting Laurent polynomials in $T^{1/2}$ to the discrete MC data $B_n(T_\tau)$ is not feasible. Therefore, adopting the procedure suggested by Schultz and Kofke,[52] we fit asymptotic forms to the low- and high-temperature limits and interpolate the residuals with Akima splines to obtain smooth dependencies on T.[52] To verify this approach, we then compute B_2 to B_6 at 625 and 875 K as well as at all temperatures $(T_\tau + T_{\tau+1})/2$ as described above. The Akima interpolant of the first MC data set reproduces this second control data set within its error estimate over the entire temperature range of interest.

3. VIRIAL COEFFICIENTS

Figure 2 shows the temperature dependence of the virial coefficients B_2 to B_6 for reduced temperatures $T^* = k_B T/\varepsilon$ between 0.5 and 5.0. Plotting the reduced quantities $B_n^* = B_n/B_0^{n-1}$, where $B_0 = 3\pi\sigma^3 N_A/2$, allows for a more direct comparison with the prototypical case of argon,[19] which is also shown in the figure. For both Hg and Ar, we plot the pairwise-additive approximations $B_{n_2}^*$ as well.

As expected, the $B_{n_2}^*$ of mercury exhibit a dependency on the reduced temperature T^* that is qualitatively similar to the argon case.[19] This is a consequence of the similarity of the Hg and Ar two-body potentials $\Phi_2^* = \Phi_2/\varepsilon$ (shown in Figure 1). However, there are pronounced quantitative differences between the $B_{n_2}^*$ of Hg and Ar, a direct consequence of the fact that the respective two-body potentials differ by more than only the length and energy scale. In particular, as has already been discussed in section 2.2, the reduced Hg_2 potential has a much softer repulsive branch $r < \sigma$ and a less steep r dependence beyond the well minimum.

dx.doi.org/10.1021/jp412260a | J. Phys. Chem. B 2014, 118, 3392−3400

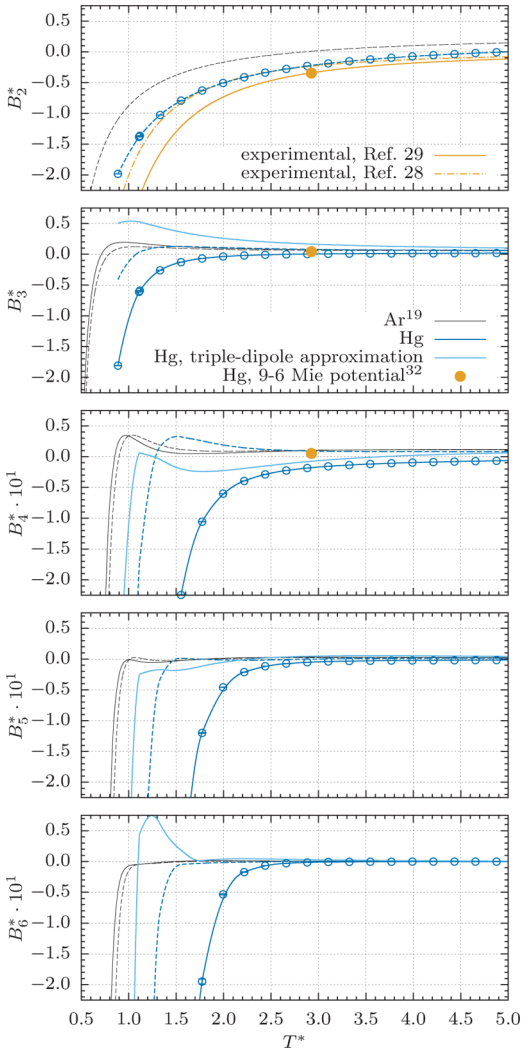

Figure 2. Reduced virial coefficients B_n^* for Hg (and Ar, taken from ref 19) as functions of temperature T. All quantities are reduced by the respective two-body potential's[38,45] σ and ε values. Empty symbols represent the calculated three-body data points and are connected by the dark-blue solid Akima interpolant; dashed curves illustrate the respective pairwise-additive approximations B_{n_2}. Also shown are the experimental B_2^* data of Hicks[29] and Busey and Giauque[28] as well as Fokin et al.'s B_2^*, B_3^*, and B_4^* values[32] at 1650 K (corresponding to T^* = 2.93).

In contrast to the Ar case, the contributions B_{n_3} of the three-body potentials to the nth virial coefficient B_n of Hg are dramatic. We note that Figure 2 somewhat exaggerates the picture by failing to account for the different length and energy scales of the Hg and Ar three-body potentials. (In the triple-dipole approximation, the single coupling parameter ω_{ddd} of the Axilrod–Teller–Muto potential is approximately $8 \times 10^3 E_h a_0^9$ for Hg as compared to about $5 \times 10^2 E_h a_0^9$ for Ar.[19,40]) Yet it is evident that the two cases are qualitatively different: with the exception of B_3, which is positive at and beyond $T^* \approx 2.75$ (i.e. 1600 K), the higher-order quantities $B_{n_2} + B_{n_3}$ are negative at all temperatures considered here. In fact, with $|B_{n_2}| < |B_{n_3}|$, the three-body parts B_{n_3} generally dominate the three-body approximations $B_{n_2} + B_{n_3}$ and diverge so strongly with decreasing T^* that we did not always obtain numerically stable results for the virial coefficients B_n at temperatures below 500 K. More specifically, this behavior is a manifestation of the nonvanishing short-range correction f_r^{EAT} of our extended Axilrod–Teller potential. The virial coefficients computed by employing the triple-dipole approximation Φ_3^{AT} (with $f_r^{AT} \equiv 0$) somewhat mimic the Ar case,[19] although the larger triple-dipole coupling parameter renders the contributions B_{n_3} substantially larger in terms of absolute magnitude. Whereas the short-range behavior of Φ_3^{EAT} is approximate as discussed in section 2.2, the large differences between the EAT and AT three-body virial coefficients B_n illustrate the importance of going beyond the triple-dipole approximation.

We close the discussion by noting that the experimental non-ideality corrections $\tilde{B}$ of Hicks[29] and Busey and Giauque,[28] such that $P(\rho, T) \approx k_B T\rho[1 + \tilde{B}(T)\rho]$, do not match the second ab initio virial coefficient of Hg.[38] It has been noted earlier that this is to be expected[29] because $\tilde{B}$ effectively captures higher terms in the density expansion of eq 1. From this point of view, the relatively good agreement of Busey's and Giauque's $\tilde{B}$ and B_2 in the T^* range of about 1.5 to 3.5 is remarkable. Also shown in Figure 2 is Fokin et al.'s computed B_2 value of −30.25 cm^3 mol^{-1} at 1650 K (about −0.35 at 2.93 in reduced units). Compared to our B_2, it is too small and indicates that the effective 9–6 Mie potential employed[32] (plotted in Figure 2) is too attractive. Fokin et al.'s B_3 and B_4 values at 1650 K do not match our ab initio data as well. Again, this is expected because Fokin et al.'s 9–6 Mie potential has been parametrized to fit a fourth-order virial EOS to experimental P–ρ–T and other data.[32] The semiempirical parametrization of ref 32 is therefore to be judged by its capability to reproduce EOS data; the "virial coefficients", being derived from a pairwise-additive effective potential as two-body integrals B_{n_2}, are of an effective nature only. We stress that the direct comparison of Fokin et al.'s[32] and our data is hindered by the somewhat approximate nature of our EAT potential as well as the missing four-body part B_{4_4}.

4. SUMMING TERMS: THE VIRIAL SERIES AND EQUATION-OF-STATE DATA

4.1. Termwise Analysis and Series Truncation. The relative absolute magnitudes of the (three-body) virial coefficients $B_{n_2} + B_{n_3} \approx B_n$ do not necessarily imply an analogous relative importance of the respective terms of the virial series. The convergence of the series of eq 1 and, eventually, the predictive capability of the EOS for a state point (ρ, T) can be assessed only by considering the interplay of the density dependence of these terms and the temperature dependence of the B_n discussed above. In ignorance of all but the first six terms of eq 1, we can clearly not speak of "convergence" of a sequence of polynomials

$$P_m(\rho, T) = k_B T\rho\left[1 + \sum_{n=2}^{m} B_n(T)\rho^{n-1}\right] \quad (5)$$

with increasing m. We would, however, expect the individual terms $|k_B T B_n(T)\rho^n|$ to grow smaller with increasing order n.

It is therefore interesting to observe that, for $n > 2$, $|B_n(T)|\rho^n$ grows larger with increasing order n over essentially the entire nontrivial density range, $\rho > 0.5$ g cm^{-3}, for $T = 500$ K. Specifically, the fourth-order term is of substantially larger absolute magnitude than the preceding third-order term and so forth. Because the B_n are density-independent, the difference

dx.doi.org/10.1021/jp412260a | J. Phys. Chem. B 2014, 118, 3392–3400

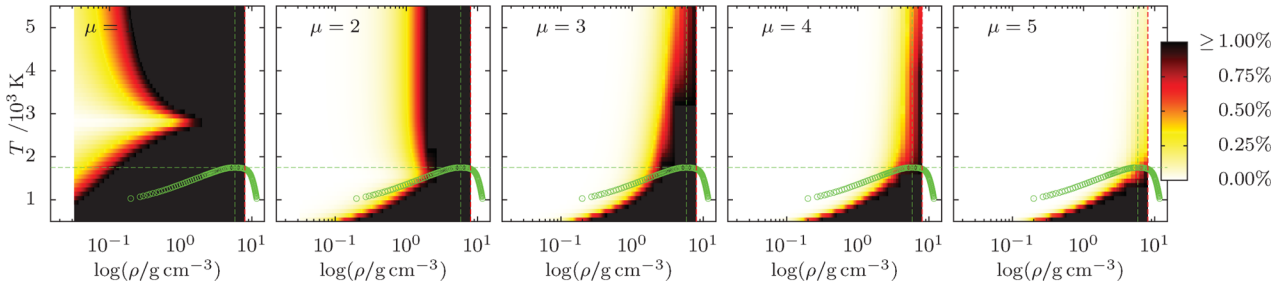

Figure 3. Remainder sum $k_B T\Sigma_{n=\mu+1}^{6}|B_n(T)|\rho^n$ relative to $Q_6(\rho,T) = k_B T\rho[1 + \Sigma_{n=2}^{6}|B_n(T)|\rho^{n-1}]$, in percent, as explained in the text. The leftmost plot with $\mu = 1$ corresponds to the ideal-gas case. Beyond 8 g cm^{-3} (i.e., to the right of the red dashed line), the sixth-order three-body virial EOS evaluates to negative pressures; the corresponding areas in the plot have been left blank. For clarification of the location in the density−temperature plane, the experimental liquid−vapor binodal and critical coordinates[4,5] are shown in green.

between the terms rapidly grows larger with increasing ρ as a direct manifestation of the relative absolute magnitudes of the B_n. With temperatures increasing from 500 K, the density range in which the term of order $n + 1$ drops below the preceding nth-order term (absolute magnitudes implied) grows larger. This is a reflection of $|B_n|$ growing smaller with increasing T and doing so more rapidly for higher orders n, as shown in Figure 2. However, we do not obtain monotonically decreasing terms over reasonable density ranges until rather high temperatures are reached. For example, at 2 g cm^{-3} and 1650 K we have

$$P/\text{MPa} = 136.7857 - 26.3502 + 0.3666 - 1.6242$$

with fifth- and sixth-order terms of −0.3944 and −0.0881, respectively. Again, comparison to Fokin et al.'s findings[32]

$$P/\text{MPa} = 136.7857 - 41.2546 + 4.4874 + 0.4840$$

is difficult because of the effective nature of the underlying semiempirical 9−6 Mie potential.[32] Note that our ab initio B_3 is crossing zero near 1600 K ($T^* = 2.75$). From this point of view, it is perhaps not very significant that the fourth-order term is of a larger absolute magnitude at this state point. However, we find similar situations for similar densities and yet higher temperatures, suggesting that the absolute magnitudes of our three-body approximations to the higher-order virial coefficients B_n are too large.

We illustrate the global picture as follows. Similar to Kofke et al.,[20,53] we do not consider P_m of eq 5 but rather the related quantities $Q_m(\rho, T) = k_B T\rho[1 + \Sigma_{n=2}^{m}|B_n(T)|\rho^{n-1}]$. Although Q_m, of course, is not the mth-order virial EOS pressure P_m, the dependence of both Q_m and P_m on the truncation order m can be discussed along similar lines. In Figure 3 we plot the remainder sum $Q_m(\rho, T) - Q_\mu(\rho, T) = k_B T\,\Sigma_{n=\mu+1}^{m}|B_n(T)|\rho^n$, expressed as a percent fraction of Q_m for $m = 6$ in the $\rho-T$ plane. In the limit $m \to \infty$, Figure 3 would plot the importance of the remainder of the polynomial Q_μ relative to the full series Q_∞.

Generally speaking, given a state point (ρ, T), the remainder sums $Q_6 - Q_\mu$ grow smaller with increasing μ. This is trivial if summing only positive terms, yet it is relevant to observe that with both decreasing density ρ and increasing temperature T a given partial sum Q_μ captures increasing portions of the reference, becoming more accurate in the sense that higher-order terms add less to the total. Even at the experimental critical coordinates of $\rho_c = 5.8$ g cm^{-3} and $T_c = 1751$ K, Q_5 approximates Q_6 better than to within 1%. This picture is somewhat similar to the cases of argon[19] and simple model systems.[52,53] However, from a consideration of Figure 3 alone, it is easy to miss the observation made for the relative absolute magnitudes of individual terms of eq 1 at comparatively lower temperatures. This regime, with higher-order terms exceeding lower-order terms in absolute magnitude, is manifested as a sharply defined, essentially μ-independent region of poor accuracy well inside the binodal. There, Q_6 is dominated by higher-order terms; $Q_{\mu+1}$ is not a significant improvement over Q_μ for lesser truncation orders μ.

We stress that Figure 3 is not indicative of the accuracy of the mth-order virial EOS. This is because the reference is not the experimental pressure or even the true sixth-order virial EOS, but a three-body approximation to it. In fact, we find our sixth-order, three-body virial EOS to be unstable and grossly inaccurate for all but very small densities. In lieu of true m-body estimates of Q_m or P_m, comparison with experimental EOS data[4,5] is perhaps the best way to illustrate the point.

4.2. Comparison to Experimental EOS Data. Figure 4 compares the sixth-order two-body and three-body virial EOSs with the experimental EOS data set of Götzlaff[4,5] for temperatures between 1500 and 3000 K. The experimental isotherms have been derived from linear isochores $P(\rho_t, T) = \gamma_V(\rho_t)T + P_i(\rho_t)$ using Götzlaff's tension coefficients γ_V and internal pressures P_i tabulated for densities ρ_t between 0.2 and 12.8 g cm^{-3}.[4]

It is evident that the sixth-order, two-body, pairwise-additive virial EOS is inaccurate for all but the smallest densities. At 1 g cm^{-3}, the 3000 K isotherm predicts a pressure of 126.7 MPa, off the experimental reference[4,5] of 125.8 MPa by about 1%. Considering that the ideal-gas model predicts a pressure of 124.4 MPa, the trend of the two-body virial EOS to systematically larger pressures, indicative of an interaction model that is too repulsive, is apparent even under these nearly ideal conditions.

Including the three-body parts $k_B T B_{n_3}(T)\rho^n$ changes the picture dramatically. Similar to the two-body, pairwise-additive case, the sixth-order, three-body virial EOS is inaccurate at all but comparatively small densities and, in fact, ill-behaved beyond. In the small-density regime, however, we find the agreement with experimental EOS data to be substantially improved with respect to the two-body approximation. For $\rho <$ 2 g cm^{-3}, deviations are positive, do not exceed 10 MPa, and decrease with increasing temperature. For example, at 2 g cm^{-3}, the 3000 K isotherm predicts a pressure that is about 0.2 MPa off the experimental reference of 255.1 MPa.[4,5] This is considerably more accurate than the ideal-gas value of 248.7 MPa, yet we feel that this level of agreement is rather to be attributed to the correct small-density (and high-temperature) limiting behavior of eq 5. The regime of nontrivial predictive capability of the sixth-order, three-body virial EOS seems to be

dx.doi.org/10.1021/jp412260a | J. Phys. Chem. B 2014, 118, 3392−3400

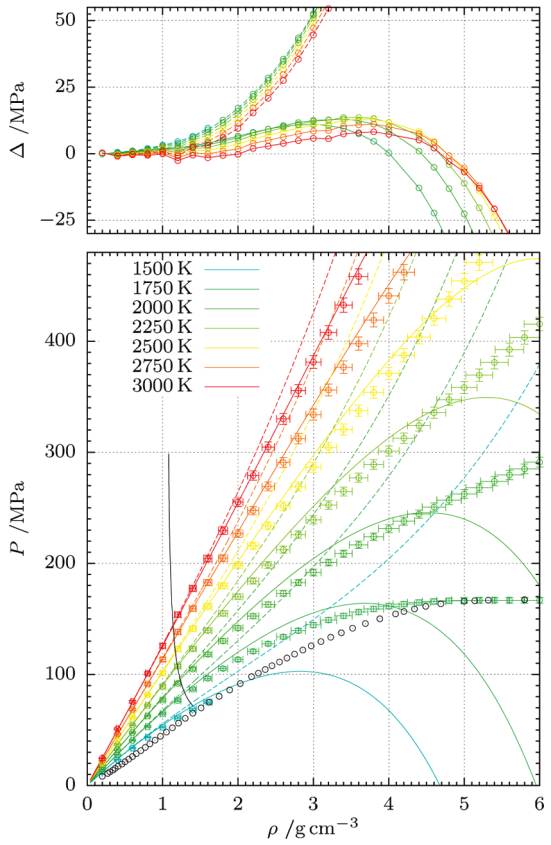

Figure 4. Comparison of experimental and ab initio $P-\rho-T$ data from the sixth-order, three-body virial EOS between 1500 and 3000 K. Solid and dashed lines are our computed three-body and two-body isotherms $P_6(\rho, T)$, respectively. Colored open symbols represent Götzlaff's experimental data sets with worst-case error estimates;[4,5] black open symbols indicate the experimental liquid–vapor coexistence line.[4,5] The (pointwise-defined) difference Δ between ab initio and experimental data is shown in the top panel. In the lower panel, the mean free path is larger than $12.5a_0$ left of the solid black line as discussed in the text.

restricted to the small-density range and temperatures perhaps not very much larger than T_c = 1751 K.[4,5] For example, at 2 g cm^{-3} and 1650 K, our sixth-order, three-body pressure is 108.7 MPa, in reasonable agreement with Fokin et al.'s fourth-order semiempirical virial EOS pressure of 100.5 MPa[32] and Götzlaff's experimental value of 102.1 MPa.[4,5] The ideal-gas model evaluates to 136.8 MPa.

Whereas we could argue that the existence of such a regime (i.e., where the gas-phase behavior is nonideal but our sixth-order three-body virial EOS is reasonably well-behaved) suggests that our ab initio approach is in principle correct, Figure 4 illustrates the fact that our EOS fails spectacularly beyond a very limited density range. All sixth-order, three-body isotherms up to 7750 K are unstable and diverge to negative pressures with increasing density. Consequently, we cannot solve $(\partial P_m/\partial\rho)_T = (\partial^2 P_m/\partial\rho^2)_T = 0$ for mth-order estimates of the critical quantities P_c, ρ_c, and T_c. (We note in passing that this is true for all $m > 3$. Only the third-order, three-body virial EOS shows van der Waals loops below, and critical behavior at, 1847.8 K.) Ultimately, this is a consequence of the fourth- and higher-order three-body virial coefficients $B_{n_2} + B_{n_3}$ being negative for all temperatures of interest. As ρ grows larger, the ideal-gas term $k_BT\rho$, or, for temperatures above 1600 K, the contribution equivalent to P_3, is dominated and eventually compensated for by negative higher-order terms. We illustrate the situation for the near-critical 1750 K isotherm in Figure 5.

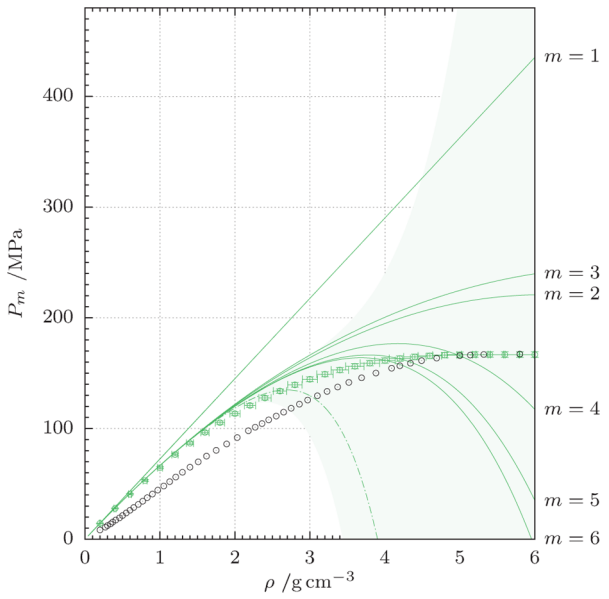

Figure 5. Isotherms as obtained from the mth-order, three-body virial EOS $P_m(\rho, T)$ for T = 1750 K. The curve for m = 1 illustrates the ideal-gas model. The dashed line is an estimated seventh-order, three-body isotherm as described in the text; the shaded area illustrates the uncertainty in P_7 arising from two standard deviations of our B_7 estimate alone. Empty teal symbols and linear splines are experimental data of Götzlaff;[4,5] black symbols mark the experimental liquid–vapor coexistence line.[4,5]

Although P_3 exhibits a van der Waals loop (outside the scale of Figure 5), successively higher orders of P_m give rise to increasingly smaller pressures for a given ρ. Consequently, evaluating P_m at the experimental critical coordinates[4,5] of 5.8 g cm^{-3} and 1751 K give monotonically smaller values of $P_m(\rho_c, T_c)$ with increasing m. In a sense, the three-body virial EOS becomes less accurate in going to higher orders; the somewhat reasonable agreement of $P_4(\rho_c, T_c)$ = 131.1 MPa with the experimental critical pressure[4,5] of 167.3 MPa is clearly fortuitous in light of Figure 5.

5. CRITICAL DISCUSSION

Whereas the great limitations of our ab initio sixth-order, three-body virial EOS are clearly evident from Figures 4 and 5, the reasons for its failure at all but very small densities are somewhat less apparent. Our data set does not allow for a definite conclusion, yet we can attempt a critical discussion in view of two (not mutually exclusive) main possibilities. Put briefly and considering the part of the fluid state space where the expansion of eq 1 is valid in the first place, our ab initio approach might fail because of the truncation of the virial series of eq 1 or because of the truncation of the many-body expansion, eq 2, of the interaction potential.

To investigate the first possibility, we have estimated a three-body approximation to the seventh-order, three-body term of eq 1. Following the computational protocol outlined in section 2, we obtain $B_{7_2} + B_{7_3} = (-10.61 \pm 14.92) \times 10^9$ cm^{18} mol^{-6} at 1750 K as an average over 9 runs of 10^{10} MC cycles each. This allows for a rough estimate of the order of magnitude, yet it is

dx.doi.org/10.1021/jp412260a | J. Phys. Chem. B 2014, 118, 3392−3400

not even accurate enough to fix the sign. From Figure 5, it is tempting to speculate that the seventh-order isotherm lies closely below $P_6(\rho,T)$, suggesting that our B_7 estimate has too large of an absolute magnitude. However, the large statistical uncertainty illustrated in Figure 5 prohibits definite conclusions. We could, of course, refine our B_7 estimate by performing more independent MC runs, but the overall picture does not suggest that higher-order terms of (the three-body approximation to) eq 1 result in improved accuracy or a larger range of applicability. In fact, the situation seems similar to the soft-sphere virial EOS recently discussed by Barlow et al.[22] For sufficiently penetrable potentials $E(\mathbf{R}^N) = \Sigma_{i<j}\varepsilon(\sigma/r)^\kappa$, large parts of the fluid state space are dominated by the asymptotic, large-density behavior of the model, corresponding to a small convergence radius of eq 1.[22] The large-density limit of the soft-sphere compression factor $Z = P/k_BT\rho$ is proportional to $\rho^{\kappa/3}$,[54,55] but eq 5 implies $Z_m \propto \rho^{m-1}$ as $\rho \to \infty$. Given the comparatively soft nature of the Hg two-body potential,[38] being softened further for $N > 2$ by the EAT three-body potential as discussed in section 2.2, it is reasonable to think that the slow convergence of eq 5 with increasing m, as observed here for the respective three-body approximations, is a real feature of mercury. A numerical evaluation of higher-order virial coefficients does not seem sensible then.

Such an endeavor seems even less promising considering the approximate nature of our three-body interaction model. There is evidence that, for the Lennard-Jones (LJ) and LJ-like systems, not all higher-order B_n are strictly positive or negative for all temperatures.[19,20,56,57] Comparison to the mercury case, with higher-order, three-body virial coefficients being negative throughout, should of course be exercised with caution; Hg is not LJ-like. However, both the apparent nonconvergence of terms $k_BTB_n(T)\rho^n$ at somewhat lower temperatures and the overall instability of the three-body isotherms suggest the possibility that our B_n are not correct in the sense that we miss higher-order, many-body parts B_{n_ν} with $\nu > 3$. We have estimated the four-body part B_{4_4} of $B_4 = B_{4_2} + B_{4_3} + B_{4_4}$ from a quadruple−dipole potential[58,59] as outlined in ref 60. We assume a quadruple−dipole coupling parameter[61] of $\omega_{\mathrm{dddd}} \approx -15\alpha^2C_6/64 = -107.146\ \mathrm{k}E_\mathrm{h}a_0^{12}$ with a highly accurate ab initio value for the polarizability α of Hg[62] and $C_6 = 392E_\mathrm{h}a_0^6$ being the dipole−dipole coefficient.[38,63] Although B_{4_4} has been shown to be insignificant for rare gases,[40,60] we find mercury's B_{4_4} to be negative and to exceed the statistical uncertainty of our MC estimates. For example, at 1750 K, we obtain $B_4 = -10\,756 \pm 29\ \mathrm{cm}^9\ \mathrm{mol}^{-3}$; conversely, $B_{4_2} + B_{4_3} = -10\,511 \pm 22\ \mathrm{cm}^9\ \mathrm{mol}^{-3}$. Similar to the triple-dipole approximation of the B_{n_3}, this is most likely a crude approximation of B_{4_4} only. However, we believe that the magnitude of the quadruple−dipole B_{4_4} estimate indicates the importance of four-body contributions for a quantitative picture.

We feel that this second point (i.e., the truncation of eq 2 at third order) is the leading cause of the problems encountered here. We therefore did not attempt to construct asymptotically consistent Padé approximants as suggested by Barlow et al.,[22] an approach with demonstrated predictive capability also beyond the radius of convergence of the soft-sphere truncated virial EOS.[22] Such approximants can hardly be expected to be successful if the underlying ab initio virial coefficients B_n are incorrect. Although our observations of sections 3 and 4 clearly put forward a negative answer to the initial question of this work—"can an ab initio three-body virial equation describe the mercury gas phase?"—they would also support the idea that a poorly converging many-body expansion of E (eq 2) effects a breakdown of the density expansion of eq 1. However, this line of reasoning gives rise to a somewhat more well-defined boundary of applicability of our sixth-order, three-body virial EOS. Assuming a Maxwellian velocity distribution for the gas phase, the mean free path is given by $l = k_BT/2^{1/2}\pi d^2P$, where d is an effective atomic diameter. If we require $l > 12.5a_0$, the Hg−Hg separation where $\mathcal{E}(\mathbf{R}^3)$ of the equilateral Hg_3 system is dispersion-dominated, we can solve the mean free path expression to find a $P-T$ regime where the third-order approximation to eq 2 is sufficient (i.e., a three-body approximation to eq 1 is acceptable). Taking d as σ_{Hg}[38] and solving eq 1 to sixth order for ρ, we obtain the region indicated in Figure 4. This is a much more conservative bound than restricting ρ to about 2 g cm^{-3} or less, as estimated in section 4.2 from comparison to experimental EOS data. At 1650 K, for example, $l > 12.5a_0$ corresponds to $\rho < 1.3$ g cm^{-3}. There the three-body approximation to P_6 evaluates to 78.8 MPa. Fokin et al.[32] and Götzlaff[4,5] find 74.0 and 76.1 MPa, respectively, whereas the ideal-gas model yields 90.7 MPa. However, such a mean free path criterion does not establish a regime of applicability of a truncated virial EOS, particularly because it does not depend on the truncation order m. In fact, eq 1 to sixth order seems to give reasonable EOS data beyond the $l > 12.5a_0$ boundary. It does, however, sketch a region of the fluid state space where we can expect our ab initio approach to be valid.

6. CONCLUSIONS AND OUTLOOK

We have demonstrated that an ab initio three-body interaction model for mercury, defined by two-body[38] and three-body potentials fitted to highly accurate Hg_2 and Hg_3 PESs, respectively, gives rise to a sixth-order, three-body virial EOS for the mercury gas phase that is in reasonable agreement with experimental data[4,5] in a limited small-density range. Using a Mayer sampling MC method[13,16,19] to numerically evaluate the virial coefficients B_2 to B_6 from this interaction model renders our B_n data free from empirical information. The achieved level of agreement is therefore on physical, not empirical grounds. In this density range, restricted to about $\rho < 1.4$ g cm^{-3} at 1500 K and somewhat less for larger temperatures, we can cautiously give a positive answer to the question initially raised here: the idea of a density expansion such as eq 1, generally taken for granted, appears to be valid. From this point of view, our observations can be thought to support the idea of referring to mercury as a "pseudonoble gas".[7]

Beyond, however, lies a regime where our ab initio sixth-order, three-body virial EOS fails spectacularly. We find the fourth-order term of eq 1 to be of larger absolute magnitude than the preceding third-order term (and similar behavior for higher orders) over a range of temperatures and densities. Generally, fourth- and higher-order terms are of large absolute magnitudes, negative, and sum to unstable isotherms that diverge to negative pressures with increasing density. We believe this to indicate the importance of higher-order terms in the many-body expansion of the interaction potential and conjecture that every term in the virial EOS is to be evaluated from the full n-body interaction. Therefore, we conclude with a

dx.doi.org/10.1021/jp412260a | J. Phys. Chem. B 2014, 118, 3392−3400

generally negative answer: a three-body virial EOS is incapable of describing the mercury gas phase.

Our conjecture can, in principle, be put to the test directly. However, employing n-body potentials to sufficiently high order will relatively soon become too demanding computationally, rendering a many-body expansion of the interaction potential E impractical: an m-body interaction model formally scales as N^m with the number of particles. Another possibility, suggested by Singh and Kofke,[16] is to couple an ab initio electronic structure method directly to a Mayer sampling MC integrator.[13,16,19] Given the large number of MC cycles needed to achieve accurate averages of higher-order B_n, interfacing Coupled-Cluster-level codes does not seem to be feasible computationally. Density functional methods are less demanding, but despite recent progress[64,65] struggle to capture van der Waals-type interactions to reliable accuracies.[10,64,66] A promising alternative, following Kitamura and others,[67,68] is a diatomics-in-molecules ansatz demonstrated to be of satisfactory accuracy for few-atom Hg_N clusters[68−70] and mercury's liquid−vapor equilibrium.[71,72] It is, however, not clear how large the number of mercury atoms need to be to reach experimental accuracy in such simulations.

We plan to continue our investigations of the virial EOS of mercury along these lines. If all of these approaches fail, then this probably implies that successfully simulating the mercury gas phase would require Monte Carlo or molecular dynamics techniques that employ the full N-body interaction potential, a computationally daunting task.

■ ASSOCIATED CONTENT

Supporting Information

Fit parameters for the AT and EAT three-body potentials as described in section 2.2. This material is available free of charge via the Internet at http://pubs.acs.org.

■ AUTHOR INFORMATION

Corresponding Authors

*E-mail: j.wiebke@massey.ac.nz.

*E-mail: p.a.schwerdtfeger@massey.ac.nz.

Notes

The authors declare no competing financial interest.

■ REFERENCES

(1) Holleman, A. F.; Wiberg, N. *Lehrbuch der Anorganischen Chemie*, 102nd ed.; de Gruyter: Berlin, 2007.

(2) Schulte, O.; Holzapfel, W. B. *Phys. Rev. B* **1996**, *53*, 569−580.

(3) Marsh, K. N. *IUPAC: Recommended Reference Materials for the Realization of Physicochemical Properties.*; Blackwell Scientific Publications: Oxford, U.K., 1987.

(4) Götzlaff, W. Ph.D. Thesis, University of Marburg, 1988.

(5) Götzlaff, W.; Schönherr, G.; Hensel, F. *Z. Phys. Chem. Neue Folge* **1988**, *156*, 219−224.

(6) Hensel, F. In *The Metal-Nonmetal Transition in Fluid Mercury: Landau-Zeldovich Revisited*; Redmer, R., Hensel, F., Holst, B., Eds.; Springer: New York, 2010; pp 23−35.

(7) Norrby, L. J. *J. Chem. Educ.* **1991**, *86*, 110−113.

(8) Pahl, E.; Schwerdtfeger, P. In *Mercury: From Atoms to Solids*; Sattler, K., Ed.; CRC Press: New York, 2010; Vol. 2, pp 3-1−3-13.

(9) Calvo, F.; Pahl, E.; Wormit, M.; Schwerdtfeger, P. *Angew. Chem., Int. Ed.* **2013**, *52*, 7583−7585.

(10) Gaston, N.; Schwerdtfeger, P. *Phys. Rev. B* **2006**, *74*, 024105-1−024105-12.

(11) Mayer, J. E.; Mayer, M. G. *Statistical Mechanics*; John Wiley & Sons: New York, 1940.

(12) Mason, E. A.; Spurling, T. H. *The Virial Equation of State*; Pergamon Press: Oxford, U.K., 1969.

(13) Hellmann, R.; Bich, E. *J. Chem. Phys.* **2011**, *135*, 084117-1−084117-7.

(14) Wheatley, R. J. *Phys. Rev. Lett.* **2013**, *110*, 200601-1−200601-4.

(15) Ree, F. H.; Hoover, W. G. *J. Chem. Phys.* **1964**, *41*, 1635−1645.

(16) Singh, J. K.; Kofke, D. A. *Phys. Rev. Lett.* **2004**, *92*, 220601-1−220601-4.

(17) Schultz, A. J.; Barlow, N. S.; Chaudhary, V.; Kofke, D. A. *Mol. Phys.* **2013**, *111*, 535−543.

(18) Benjamin, K. M.; Schultz, A. J.; Kofke, D. A. *J. Phys. Chem. B* **2009**, *113*, 7810−7815.

(19) Jäger, B.; Hellmann, R.; Bich, E.; Vogel, E. *J. Chem. Phys.* **2011**, *135*, 084308-1−084308-12.

(20) Schultz, A. J.; Kofke, D. A. *Mol. Phys.* **2009**, *107*, 2309−2318.

(21) Clisby, N.; McCoy, B. M. *J. Stat. Phys.* **2006**, *122*, 15−57.

(22) Barlow, N. S.; Schultz, A. J.; Weinstein, S. J.; Kofke, D. A. *J. Chem. Phys.* **2012**, *137*, 204102-1−204102-13.

(23) Masters, A. J. *J. Phys.: Condens. Matter* **2008**, *20*, 283102.

(24) Ushcats, M. V. *Phys. Rev. Lett.* **2012**, *109*, 040601-1−040601-4.

(25) Ushcats, M. V. *Phys. Rev. E* **2013**, *87*, 042111-1−042111-6.

(26) Jäger, B. *Z. Phys. Chem.* **2013**, *227*, 303−314.

(27) Wiebke, J.; Senn, F.; Pahl, E.; Schwerdtfeger, P. *J. Chem. Phys.* **2013**, *138*, 071105-1−071105-4.

(28) Busey, R. H.; Giauque, W. F. *J. Am. Chem. Soc.* **1953**, *75*, 806−809.

(29) Hicks, W. T. *J. Chem. Phys.* **1963**, *38*, 1873−1880.

(30) Cordes, H.; Dost, L.; Cammenga, H. K. *Z. Metallkd.* **1971**, *62*, 915−925.

(31) Apfelbaum, E. M.; Vorob'ev, V. S.; Martynov, G. A. *Chem. Phys. Lett.* **2005**, *413*, 342−345.

(32) Fokin, L. R.; Popov, V. N.; Naurzakov, S. P. *High Temp.* **2011**, *49*, 832−840.

(33) Moyano, G. E.; Wesendrup, R.; Söhnel, T.; Schwerdtfeger, P. *Phys. Rev. Lett.* **2002**, *89*, 103401-1−103401-4.

(34) Hermann, A.; Krawczyk, R. P.; Lein, M.; Schwerdtfeger, P.; Hamilton, I. P.; Stewart, J. J. P. *Phys. Rev. A* **2007**, *76*, 013202-1−013202-10.

(35) Selin, N. E. *Annu. Rev. Environ. Resour.* **2009**, *34*, 43−63.

(36) Zheng, Y.; Jensen, A. D.; Windelin, C.; Jensen, F. *Prog. Energy Combust.* **2012**, *38*, 599−629.

(37) Zahir, F.; Rizwi, S. J.; Haq, S. K.; Khan, R. H. *Environ. Toxicol. Pharmacol.* **2005**, *20*, 351−360.

(38) Pahl, E.; Figgen, D.; Thierfelder, C.; Peterson, K. A.; Calvo, F.; Schwerdtfeger, P. *J. Chem. Phys.* **2010**, *132*, 114301-1−114301-6.

(39) Wiebke, J.; Schwerdtfeger, P.; Moyano, G. E.; Pahl, E. *Chem. Phys. Lett.* **2011**, *514*, 164−167.

(40) Wiebke, J.; Schwerdtfeger, P.; Pahl, E. *J. Chem. Phys.* **2012**, *137*, 064702-1−064702-8.

(41) Werner, H.-J. et al. *MOLPRO*, version 2012.1, *a package of ab initio programs*, 2012; see http://www.molpro.net.

(42) Figgen, D.; Rauhut, G.; Dolg, M.; Stoll, H. *Chem. Phys.* **2005**, *311*, 227−244.

(43) Peterson, K. A.; Puzzarini, C. *Theor. Chem. Acc.* **2005**, *114*, 283−296.

(44) Helgaker, T.; Klopper, W.; Koch, H.; Noga, J. *J. Chem. Phys.* **1997**, *106*, 9639−9646.

(45) Jäger, B.; Hellmann, R.; Bich, E.; Vogel, E. *Mol. Phys.* **2009**, *107*, 2181−2188.

(46) Schwerdtfeger, P.; Assadollahzadeh, B.; Hermann, A. *Phys. Rev. B* **2010**, *82*, 205111-1−205111-11.

(47) Lotrich, V. F.; Szalewicz, K. *J. Chem. Phys.* **1997**, *106*, 9688−9702.

(48) Malijevský, A.; Karlický, F.; Kalus, R.; Malijevský, A. *J. Phys. Chem. C* **2007**, *111*, 15565−15568.

(49) Gardner, P. J.; Pang, P.; Preston, S. R. *J. Chem. Eng. Data* **1991**, *36*, 265−268.

(50) Röpke, G.; Nagel, S.; Redmer, R. *Contrib. Plasma Phys.* **1993**, *33*, 441−448.

(51) Poling, B. E.; Prausnitz, J. M.; O'Connell, J. P. *The Properties of Gases and Liquids*, 5th ed.; McGraw-Hill Professional: New York, 2000.
(52) Schultz, A. J.; Kofke, D. A. *Mol. Phys.* **2009**, *107*, 1431−1436.
(53) Tan, T. B.; Schultz, A. J.; Kofke, D. A. *Mol. Phys.* **2011**, *109*, 123−132.
(54) Song, Y.; Mason, E. A. *Phys. Rev. A* **1991**, *44*, 8400−8402.
(55) Heyes, D. M.; Clarke, S. M.; Brańka, A. C. *J. Chem. Phys.* **2009**, *131*, 204506-1−204506-11.
(56) Vompe, A. G.; Martynov, G. A. *J. Chem. Phys.* **1997**, *106*, 6095−6101.
(57) Apfelbaum, E. M.; Vorob'ev, V. S.; Martynov, G. A. *J. Chem. Phys.* **2007**, *127*, 064507-1−064507-5.
(58) Bade, W. L. *J. Chem. Phys.* **1957**, *27*, 1280−1284.
(59) Bade, W. L. *J. Chem. Phys.* **1958**, *28*, 282−284.
(60) Wiebke, J.; Pahl, E.; Schwerdtfeger, P. *J. Chem. Phys.* **2012**, *137*, 014508-1−014508-7.
(61) Johnson, C. H. J.; Spurling, T. H. *Aust. J. Chem.* **1974**, *27*, 241−247.
(62) Pershina, V.; Borschevsky, A.; Eliav, E.; Kaldor, U. *J. Chem. Phys.* **2008**, *128*, 024707-1−024707-9.
(63) Tang, K. T.; Toennies, J. P. *Mol. Phys.* **2008**, *106*, 1645−1653.
(64) Cramer, C. J.; Truhlar, D. G. *Phys. Chem. Chem. Phys.* **2009**, *11*, 10757−10816.
(65) Björkmann, T.; Gulans, A.; Krasheninnikov, A. V.; Nieminen, R. M. *J. Phys.: Condens. Matter* **2012**, *24*, 424218-1−424218-11.
(66) Gaston, N.; Paulus, B.; Rosciszewski, K.; Schwerdtfeger, P.; Stoll, H. *Phys. Rev. B* **2006**, *74*, 094102-1−094102-9.
(67) Kitamura, H. *Chem. Phys.* **2006**, *325*, 207−219.
(68) Calvo, F.; Pahl, E.; Schwerdtfeger, P.; Spiegelman, F. *J. Chem. Theory Comput.* **2012**, *8*, 639−648.
(69) Kitamura, H. *Chem. Phys. Lett.* **2006**, *425*, 205−209.
(70) Kitamura, H. *Eur. Phys. J. D* **2007**, *43*, 33−36.
(71) Kitamura, H. *J. Chem. Phys.* **2007**, *126*, 134509-1−134509-8.
(72) Kitamura, H. *J. Phys.: Condens. Matter* **2007**, *19*, 072102-1−072102-7.